

Schizophrenia Risk Proteins ZNF804A and NT5C2 Interact at Synapses

Afra Aabdien^{1,2}, Laura Sichlinger^{1,2}, Nicholas J.F. Gattford^{1,2}, Pooja Raval^{1,2},
Madeleine R. Jones^{1,2}, Lloyd Tanangonan^{1,2}, Timothy R. Powell^{3,4}, Rodrigo R.R.
Duarte^{3,4}, Deepak P. Srivastava^{1,2*}

¹Department of Basic and Clinical Neuroscience, The Maurice Wohl Clinical
Neuroscience Institute, Institute of Psychiatry, Psychology, & Neuroscience, King's
College London, London, UK.

²MRC Centre for Neurodevelopmental Disorders, Institute of Psychiatry, Psychology
and Neuroscience, King's College London, London; United Kingdom.

³Social, Genetic & Developmental Psychiatry Centre, Institute of Psychiatry,
Psychology & Neuroscience, King's College London, London, United Kingdom.

⁴Department of Medicine, Weill Cornell Medical College, Cornell University, New
York, NY, USA.

*** = corresponding author: deepak.srivastava@kcl.ac.uk**

26 **ABSTRACT**

27 The zinc finger protein 804A (*ZNF804A*) and the 5'-nucleotidase cytosolic II
28 (*NT5C2*) genes have been identified as robust susceptibility genes in large-scale
29 genome-wide association studies of schizophrenia. The *ZNF804A* and *NT5C2*
30 proteins are highly expressed in developing and mature cortical neurons. *ZNF804A*
31 has been implicated in regulating the development of neuronal morphology; it localises
32 to synapses and is required for activity-dependent modifications of dendritic spines.
33 *NT5C2* has been shown to regulate 5' adenosine monophosphate-activated protein
34 kinase activity and implicated in influencing protein synthesis in neural progenitor cells.
35 But despite these findings, a better understanding of the role these proteins play in
36 regulating neuronal function is needed. A recent yeast two-hybrid screen has identified
37 *ZNF804A* and *NT5C2* as potential interacting proteins, but whether this occurs *in situ*;
38 and moreover, in cortical neurons, is unknown. Here we show that *ZNF804A* and
39 *Nt5c2* colocalise and interact in hEK293T cells. Furthermore, their rodent
40 homologues, *ZFP804A* and *NT5C2*, specifically colocalise at synapses and form a
41 protein complex in cortical neurons. Knockdown of *Zfp804A* or *Nt5c2* resulted in a
42 significant decrease in synaptic expression of both proteins, suggesting that both
43 proteins are required for the synaptic targeting of each other. Taken together, these
44 data indicate that *ZNF804A/ZFP804A* and *NT5C2* interact together in cortical neurons
45 and indicate that these GWAS risk factors may function as a complex to regulate
46 neuronal function.

47

48 **Keywords:** Psychosis, dendritic spine, dendrite, *ZNF804A*, *NT5C2*.

49 INTRODUCTION

50 Schizophrenia is a chronic psychiatric disorder of complex aetiology (Birnbaum
51 and Weinberger, 2017; Lewis and Levitt, 2002; Rapoport et al., 2012; Smeland et al.,
52 2020). Genome-wide association studies (GWAS) have suggested up to one third of
53 genetic risk for schizophrenia arises from common alleles (Ripke et al., 2011) and the
54 latest study has identified 270 independent schizophrenia risk loci (Ripke et al., 2020).
55 The zinc finger protein 804A (*ZNF804A*) and the 5'-nucleotidase, cytosolic II (*NT5C2*,
56 *cN-II*) genes were amongst the first ones to emerge from early GWAS of schizophrenia
57 (O'Donovan et al., 2008; Ripke et al., 2011), and they have also been implicated in
58 susceptibility to multiple psychiatric disorders (Amare et al., 2019; Cross-Disorder
59 Group of the Psychiatric Genomics Consortium, 2013; Williams et al., 2011).
60 Transcriptome-wide association studies (TWAS) have also associated *ZNF804A*
61 (Gandal et al., 2018) and *NT5C2* (Hall et al., 2020) with schizophrenia. Ultimately,
62 schizophrenia risk variants are associated with reduced expression of *NT5C2* (Duarte
63 et al., 2016; Hall et al., 2020) and *ZNF804A* in the foetal and adult brain (Hill and Bray,
64 2012; Tao et al., 2014), but the function of these proteins in mature neurons remains
65 unclear.

66 The *ZNF804A* protein has been found to be expressed in the human cerebral
67 cortex, particularly in pyramidal neurons (Tao et al., 2014). *ZNF804A* has also been
68 found to localise to putative synapses, as demonstrated by co-localisation with the
69 synaptic proteins PSD-95 and GluN1 (Deans et al., 2017). Similarly, *ZFP804A* (rodent
70 homologue) was found to be enriched in synaptic fractions, and to localise to dendritic
71 spines, where the majority of excitatory synapses occur in the mammalian brain
72 (Deans et al., 2017). Consistent with a role for the encoded zinc finger protein at
73 synapses, knockdown or knockout of *Zfp804A* resulted in a reduction of dendritic spine

74 density (Deans et al., 2017; Huang et al., 2020), whereas an increase in spine density
75 was observed when the full length or shorter disease-associated isoform of the protein
76 was overexpressed in cortical neurons (Dong et al., 2021; Zhou et al., 2020).
77 Moreover, activity-dependent remodelling of dendritic spines was impaired in cortical
78 neurons with reduced ZNF804A expression levels (Deans et al., 2017). Together,
79 these data indicate a role for ZNF804A at synapses.

80 The NT5C2 protein also appears to be enriched in cortical neurons (Duarte et
81 al., 2019), but relative to ZNF804A, less is known about the function of NT5C2 in the
82 cortex. The knockdown of *NT5C2* in human neural progenitor cells is associated with
83 increased phosphorylated 5' adenosine monophosphate-activated protein kinase
84 (AMPK), which negatively regulates mammalian target of rapamycin (mTOR) and
85 eukaryotic elongation factor 2 (eEF2), suggesting a role in protein translation (Duarte
86 et al., 2019). Knockdown of *CG32549* (the *Drosophila melanogaster* homologue)
87 causes motor defects (Duarte et al., 2019), and increased sleep in flies (Singgih et al.,
88 2021). Whereas it appears that *NT5C2* has a function in the developing and adult
89 brain, the precise underlying neurological mechanisms are yet to be established.

90 A recent interactome study using a yeast two-hybrid assay has indicated that
91 ZNF804A interacts with multiple proteins, including NT5C2 (Zhou et al., 2018). Follow
92 up studies have demonstrated that ZNF804A forms a complex with several predicted
93 interactors to regulate neuronal morphology (Dong et al., 2021). Interestingly, it was
94 noted that NT5C2 is the only potential interacting protein for ZNF804A, encoded by a
95 GWAS-supported gene (Zhou et al., 2018). In this study, we investigate the subcellular
96 localisation of ZNF804A and NT5C2, and explored whether they formed a protein
97 complex in heterologous hEK293T cells and rodent cortical neurons. We find that
98 ZNF804A and NT5C2 do form a protein complex in heterologous and cortical neurons.

99 Both proteins are present in multiple subcellular compartments but co-localise at or
100 near synapses in cortical neurons. Small interfering RNA (siRNA)-mediated
101 knockdown of either protein resulted in altered presence of both proteins at synapses.
102 Together, these data support a model whereby two risk factors for schizophrenia may
103 function as a complex to regulate synaptic function.

104

105 **RESULTS**

106

107 **ZNF804A and NT5C2 form a protein complex in heterologous cells.**

108 As a yeast-two hybrid assays has revealed that ZNF804A and NT5C2 are
109 potential interacting partners (Zhou et al., 2018), we were interested in confirming this
110 *in situ*. We first examined the localisation of ectopically expressed HA-ZNF804A and
111 Myc-NT5C2 in hEK293T cells. Consistent with findings from Deans et al. (2017), HA-
112 ZNF804A localised to both nuclear and cytosolic compartments (**Figure 1A**). Within
113 the cytosol and at the plasma membrane, HA-ZNF804A co-localised with the
114 cytoskeletal filament, F-actin probe (phalloidin) (**Figure 1A**). hEK293T cells
115 transfected with Myc-NT5C2 showed that this protein mainly localised to the cytosol
116 (**Figure 1B**), consistent with findings from Duarte et al. (2019). We next co-transfected
117 HA-ZNF804A and Myc-NT5C2 into hEK293T cells and observed that HA-ZNF804A
118 and Myc-NT5C2 co-localised in the cytoplasm and near the plasma membrane of
119 hEK295T cells (**Figure 1C**). This was confirmed by a line graph construction, whereby
120 the fluorescence intensity of both proteins was measured (**Figure 1D – i & ii**), and the
121 overlap between the intensities provided evidence of co-localisation.

122 To validate these findings and further determine whether ZNF804A and NT5C2
123 formed a protein complex, we performed a co-immunoprecipitation using hEK293T
124 cells ectopically expressing both proteins. Cells co-transfected with HA-ZNF804A and
125 Myc-NT5C2 were immunoprecipitated with an anti-Myc antibody to isolate NT5C2 and
126 its interacting partners (**Figure 1E**). As expected, Myc-NT5C2 was readily detected in
127 the immunoprecipitation (IP) sample. In addition, HA-ZNF804A was also present in
128 the IP sample indicating that ZNF804A and NT5C2 were part of a protein complex
129 (**Figure 1E**). Taken together, these data indicate that ZNF804A and NT5C2 co-localise
130 in the cell cytoplasm, near the membrane, and that they form a protein complex in
131 hEK293T cells.

132

133 **Subcellular distribution of ZNF804A and NT5C2 in cortical neurons.**

134 Previous work has demonstrated that ZNF804A localises to somatodendritic
135 compartments of neurons, and particularly in dendritic spines (Deans et al., 2017). In
136 comparison, little is known about the distribution and organisation of NT5C2 in
137 neurons. We first sought to confirm the ZNF804A distribution *in vivo*, using cell
138 fractions generated from mouse cortex. Cortices were subjected to a subcellular
139 fractionation protocol yielding whole cell (non-nuclear) (P1), cytosolic (S2) and crude
140 synaptosomal (P2) subcellular fractions (Jones et al., 2014). Synaptosomal fractions
141 were further subjected to Triton-X100 detergent separation to produce a supernatant
142 (S) and precipitate (P) (Jones et al., 2014) (**Figure 2A**). Consistent with our previous
143 finding, ZFP804A was present in both cytosolic and synaptosomal fractions; however,
144 the protein was highly enriched in synaptosomal supernatant, indicating a loose
145 association with synaptic membrane (**Figure 2A**). As expected, PSD-95, a major

146 component of synapses and the post-synaptic density, was enriched in synaptosomal
147 precipitate fractions indicating a tight association with synaptic membranes (**Figure**
148 **2A**). Examination of NT5C2 distribution revealed that it was also present in cytosolic
149 and synaptosomal fractions, although it was enriched in the cytosol. NT5C2 was only
150 loosely associated with synaptic membrane as indicated by presence of the protein in
151 synaptosomal supernatant fractions (**Figure 2A**). These findings corroborate that
152 ZFP804A /ZNF804A localises to multiple subcellular compartments beyond the
153 nucleus (Deans et al., 2017), and suggest a role for NT5C2 at synapses.

154 To further investigate the subcellular localisation of ZFP804A and NT5C2, we
155 performed a series of immunostaining experiments in DIV20 (days *in vitro*) primary
156 cortical neurons. Staining for endogenous ZFP804A revealed significant enrichment
157 of this protein in the synaptic region (region adjacent to dendrite), compared to
158 dendrites (ZFP804A puncta count: Dendrite, 8.37 ± 0.32 ; Synaptic region, 14.03 ± 0.53
159 ($t(7)=9.10$, $p<0.0001$, $n=8$)) (**Figure 2B**). Staining for endogenous NT5C2 also
160 revealed significant enrichment of this protein in the synaptic region compared to
161 dendrites (NT5C2 puncta count: Dendrite, 7.01 ± 0.24 ; Synaptic region, 11.77 ± 0.45
162 ($U=214$, $p<0.0001$, $n=8$)) (**Figure 2C**). Combined, these data indicate that ZFP804A
163 and NT5C2 localise to both dendrites and synaptic regions, suggesting that both
164 proteins are present within the same subcellular compartments in neurons.

165

166 **ZNF804A and NT5C2 colocalise and interact in cortical neurons.**

167 Considering that ZNF804A and NT5C2 form a protein complex in Hek293T
168 cells, and that ZFP804A and NT5C2 localise to the same subcellular compartments in
169 cortical neurons, we sought to explore whether these proteins were part of a protein

170 complex in rat cortical neurons, *in situ*. First, we examined whether both proteins co-
171 localised together in cortical neurons. In DIV20 cortical neurons, both ZFP804A and
172 NT5C2 were found to co-localise in synaptic regions: this is demonstrated by the
173 multiple white and yellow arrows and the green/magenta overlap in the orthogonal
174 projections indicated by the orange arrows (**Figure 3A**). To further confirm this
175 synaptic colocalization, we analyzed ZFP804A puncta intensity within NT5C2 puncta
176 in synaptic regions compared to dendrites. This revealed significantly more ZFP804A
177 puncta overlapping within NT5C2 puncta in synaptic regions compared to dendrites
178 (ZNF804A puncta intensity: Dendrite, 5.16 ± 0.27 ; Synaptic region, 6.60 ± 0.44
179 ($t(7)=2.78$, $p=0.0065$, $n=8$)) (**Figure 3B**). The inverse relationship was also found to
180 be true, whereby significantly more NT5C2 puncta were found to overlap with
181 ZFP804A puncta in synaptic regions compared to dendrites (NT5C2 puncta intensity:
182 Dendrite, 7.34 ± 0.31 ; Synaptic region, 9.54 ± 0.52 ($t(7)=3.61$, $p=0.0005$, $n=8$)) (**Figure**
183 **3C**).

184 To demonstrate this colocalization represented a potential interaction between
185 the two proteins, we performed a co-immunoprecipitation assay for ZFP804A from
186 cortical neuron lysates. Consistent with our data from heterologous cells,
187 immunoblotting revealed that NT5C2 was present in lysates immunoprecipitated for
188 ZFP804A, but not for rabbit IgG (**Figure 3D**). These data indicate that ZFP804A and
189 NT5C2 colocalize near synaptic regions in cortical neurons, and that they are part of
190 a protein complex.

191

192 **Knockdown of *Zfp804a* or *Nt5c2* results in the redistribution of associated**
193 **proteins.**

194 To further investigate a functional interaction between ZFP804A and NT5C2 in
195 cortical neurons, we knocked down *Zfp804a* using a previously validated siRNA
196 (Deans et al., 2017) in DIV15 primary rat cortical neurons. We then observed the
197 effects of this knockdown on synaptic and dendritic NT5C2 localisation at DIV20. We
198 first validated the efficacy of the *Zfp804a* siRNA by quantifying the number of ZFP804A
199 puncta between *Zfp804a* siRNA knockdown, scrambled siRNA, or blank
200 (untransfected) conditions. The *Zfp804a* siRNA was shown to successfully target
201 ZFP804A as significantly fewer ZFP804A puncta were found in the siRNA knockdown
202 condition compared to both the blank and scramble conditions (puncta per 10 μ m:
203 Blank, 22.45 \pm 1.44; Scramble, 22.05 \pm 1.03; *Zfp804a* siRNA, 16.38 \pm 1.20. One-way
204 ANOVA: $F(2,47)=27.04$, $p<0.0001$, Blank/siRNA Bonferroni: ($t(5)=6.91$, $p<0.0001$,
205 $n=6$); Scramble/siRNA Bonferroni: ($t(5)=5.46$, $p<0.0001$, $n=6$)) (**Figure 4A+B**). No
206 significant difference in ZFP804A puncta were observed between the blank or
207 scramble conditions, indicating specificity of the siRNA treatment.

208 Next, we knocked down *Zfp804a* in DIV15 rat primary cortical neurons and
209 observed the effects on NT5C2 puncta in dendrites and synaptic regions of DIV20
210 cortical neurons. *Zfp804a* knockdown significantly reduced the density of NT5C2
211 puncta in synaptic regions (puncta per 10 μ m; Synaptic region: Blank, 11.78 \pm 0.93;
212 Scramble, 11.73 \pm 0.81; *Zfp804a* siRNA, 6.88 \pm 0.80. Two-way ANOVA: $F(2,102)=7.29$,
213 $p=0.0011$; Bonferroni post hoc test ($p<0.0001$, $n=6$)) (**Figure 4C+D**). In contrast, no
214 effect on NT5C2 puncta number was observed in dendrites across conditions (**Figure**
215 **4D**).

216 To further probe the nature of this functional interaction, we then performed the
217 inverse experiment to understand if *Nt5c2* expression can influence ZFP804A
218 localization. We knocked down *Nt5c2* using an siRNA previously validated (Duarte et

219 al., 2019), in DIV15 rat primary cortical neurons. We then observed the effects of the
220 knockdown on synaptic and dendritic ZFP804A localisation at DIV20, to allow for
221 sufficient protein turnover. We first validated the efficacy of two siRNAs for *Nt5c2* via
222 immunoblotting comparing between siRNA A or B knockdown, scrambled siRNA, or
223 blank (untransfected) conditions. This revealed the *Nt5c2* siRNA A successfully
224 targeted and knocked down NT5C2 in primary rat cortical neurons, as a clear decrease
225 in protein expression was observed in this condition compared to both the siRNA B,
226 blank, and scramble conditions (**Figure 5A**). No difference in NT5C2 protein
227 expression was observed between the blank or scramble conditions, indicating
228 specificity of the siRNA treatment.

229 We knocked down *Nt5c2* in DIV15 rat primary cortical neurons and observed
230 the effects on ZFP804A puncta in dendrites and synaptic regions of DIV20 rat primary
231 cortical neurons. The knockdown significantly reduced the number of ZFP804A puncta
232 in synaptic regions (puncta per 10 μm ; Synaptic region: Blank, 13.28 ± 1.34 ; Scramble,
233 12.47 ± 0.48 ; *Nt5c2* siRNA A, 6.91 ± 2.43 . Two-way ANOVA: $F(2,12)=6.07$, $p=0.0151$;
234 Bonferroni post hoc test (Blank/scramble, $p=0.0113$, $n=3$; Scramble/siRNA A,
235 $p=0.026$, $n=3$) (**Figure 5B+C**). Similar to the ZFP804A knockdown, no effect on
236 ZFP804A puncta was observed in dendrites when *Nt5c2* was knocked down. These
237 data suggest a bidirectional signalling interaction occurs between NT5C2 and
238 ZFP804A which operate in concert at synapses but not in dendrites.

239

240 DISCUSSION

241 Mutations in multiple key synaptic genes have been previously associated with
242 schizophrenia pathogenesis (Forrest et al., 2018; Penzes et al., 2011), but the precise

243 nature of how these molecules interact to impair synapses in schizophrenia is
244 unknown. *ZNF804A* and *NT5C2* are robust schizophrenia susceptibility genes (Ripke
245 et al., 2020), that have been previously suggested to interact (Zhou et al., 2018). In
246 this context, *ZNF804A* has been previously characterised as having roles in mediating
247 activity-dependent structural plasticity of dendritic spines, neurite outgrowth, protein
248 translation and gene transcription (Deans et al., 2017; Hill et al., 2012; Zhou et al.,
249 2018). *NT5C2*, in turn, is a nucleotidase that regulates AMPK signalling, and has
250 putative effects on protein translation (Duarte et al., 2019). However, the molecular
251 mechanisms underlying their association with schizophrenia, or how they relate to
252 synaptic function or to each other, remains unclear. Here, we show *ZNF804A* and
253 *NT5C2* colocalise and localise to synapses in cortical neurons, and that they are part
254 of a protein regulatory network that is able to bidirectionally regulate itself, whereby
255 expression of one protein regulates the expression of the other. This furthers our
256 understanding of the role these proteins may play at synapses, and further suggest
257 how both proteins may contribute to synaptic dysfunction in schizophrenia.

258 In this study we demonstrate that exogenous *ZNF804A* and *NT5C2* form a
259 protein complex in hEK293T cells. Further, we show that their rodent homologues,
260 *ZNF804A* and *NT5C2* are part of a protein complex in primary cortical neurons,
261 although the consequence of this interaction is unclear. One biological function that
262 both proteins appear to jointly regulate is protein translation. *ZNF804A* interacts with
263 several proteins involved in protein translation, and has been shown to regulate the
264 rate of protein synthesis in hEK293 and CAD cells (Zhou et al., 2018). *NT5C2* has also
265 been shown to regulate the activity of the 40S ribosomal protein RPS6, which is
266 associated with protein translation (Duarte et al., 2019). Based on their predicted
267 function and localization at synapses, we hypothesize that their interaction results in

268 a protein complex (formed in combination with other proteins, as described in Zhou et
269 al. (2018)) responsible for regulating local protein translation. Furthermore, defects in
270 ZNF804A or NT5C2 may contribute to dysfunctional local synaptic protein synthesis
271 in neurological disorders. Indeed, dysregulated protein synthesis has been shown in
272 schizophrenia patient-derived olfactory neuronal cells and induced pluripotent stem
273 cell-derived forebrain neural progenitor cells from schizophrenia patients (English et
274 al., 2015; Topol et al., 2015). Common genetic variants in ZNF804A or NT5C2 could,
275 therefore, be at least partly responsible for the dysregulation in protein translation
276 observed in association with schizophrenia. Future studies are warranted to explore if
277 a ZNF804A/NT5C2 protein complex could influence protein translation.

278 A second major finding in this study is the description of the subcellular
279 distribution of ZNF804A and NT5C2 in cortical neurons. Both ZNF804A and NT5C2
280 were present in multiple subcellular compartments in cortical neurons. Consistent with
281 our previous work (Deans et al., 2017), ZFP804A was present in cytosolic and
282 synaptosomal fractions from cortical neurons. Interestingly, ZFP804A was
283 predominately present in the supernatant fraction of synaptosomes following
284 detergent separation. This indicates that ZFP804A is transiently, or 'loosely',
285 associated with the synaptic membrane. NT5C2 was also present in both cytosolic
286 and synaptosomal preparations; however, this protein was more abundant in the
287 cytosolic fraction. In synaptosomal fractions, NT5C2 was also abundant in supernatant
288 fraction of synaptosomes following detergent separation. The similar distributions of
289 both proteins were further reflected by immunostaining. To note, our assessment of
290 'synaptic regions' by immunostaining as well as our subcellular fractionation protocol
291 does not distinguish protein from being present in both pre- and post-synaptic
292 compartments. Using super-resolution imaging, ZFP804A has been localised to pre-

293 synaptic terminals as well as post-synaptic dendritic spines (Deans et al., 2017). It
294 remains to be determined whether NT5C2 can be found in either, or both pre- and
295 post-synaptic compartments. Nevertheless, our data indicates that rodent NT5C2 and
296 ZNF804A colocalise in synaptic regions. Coupled with our co-immunoprecipitation
297 data, this could indicate that these two proteins functionally interact in this region.

298 A limitation of our study is that, although the knockdown of either *Zfp804A* or
299 *Nt5c2* in primary cortical neurons resulted in a loss of either protein specifically from
300 synaptic regions, it is challenging to determine whether this was caused by a direct
301 removal of the protein from synapses, or due to a loss of the synapses altogether. For
302 example, siRNA-mediated knockdown of *Zfp804A* also results in the loss of dendritic
303 spines (Deans et al., 2017). Therefore, the apparent reduction of NT5C2 in synaptic
304 regions could be driven by the fact that there are fewer dendritic spines for the protein
305 to localise to. NT5C2 can signal through AMPK; activation of this kinase has been
306 shown to induce dendritic spine loss (Mairet-Coello et al., 2013). Thus, knockdown of
307 *Nt5c2* could induce dendritic spine loss through AMPK activation. A better
308 understanding of how synaptic structures are regulated will allow us to clarify the role
309 of NT5C2 and ZNF804A proteins at synapses.

310 There is a growing appreciation of the need to understand how genetic risk
311 factors interact with each other and with environmental factors. It is posited that such
312 interactions likely shape and contribute to complex genetic disorders such as
313 schizophrenia. Recent studies have begun to dissect how different genetic risk factors
314 can act in a synergistic manner to converge on common biological processes to
315 increase risk for psychiatric disorders (Schrode et al., 2019). In this study, we
316 demonstrate that two genetic risk factors for psychiatric disorders co-localise and form
317 a protein complex at synapses, thus revealing a novel understanding of these

318 schizophrenia susceptibility genes. While additional research is required to
319 understand the function of a ZNF804A and NT5C2 protein complex, these data
320 support a model whereby genetic risk factors may directly work in a co-operative or
321 non-additive manner to increase risk for schizophrenia.

322

323 **METHODS**

324 **Cell Culture**

325 Human embryonic kidney (HEK293) cells were maintained in a 37°C/5% CO₂
326 atmosphere in DMEM:F12 (Sigma, D6421) supplemented with 10% foetal bovine
327 serum (ClonTech, 631107), 1% L-glutamine (Sigma, G7513), and 1%
328 penicillin/streptomycin (Life Technologies, 15070063). Cells were passaged and
329 plated at 30-40% confluency on 1.5H 18 mm glass coverslips 24 hours prior to
330 transfection.

331 Primary cortical neuronal cultures were harvested from pregnant Sprague-
332 Dawley rats at embryonic day 18 as described previously (Srivastava et al., 2011).
333 Animals were habituated for 3 days before experimental procedures, which were
334 carried out in accordance with the Home Office Animals (Scientific procedures) Act,
335 United Kingdom, 1986. Cells were seeded on 1.5H 13 mm glass coverslips coated
336 with poly-D-lysine 10 µg/mL (Sigma, P0899) diluted in 1X borate buffer (Thermo
337 Scientific, 28341) at a density of 3×10^5 /well equating to 857/mm². Cells were cultured
338 in feeding media: neurobasal medium (21103049) supplemented with 2% B27
339 (17504044), 0.5 mM glutamine (25030024), and 1% penicillin/streptomycin
340 (15070063) (all reagents from Life Technologies, UK). After 4 days in vitro (DIV), 200
341 µM of d,l-amino-phosphonovalerate (d,l-APV, ab120004; Abcam) was added to media

342 to maintain neuronal health over long-term culture and to reduce cell death due to
343 excitotoxicity (Srivastava et al., 2011). Fifty percent media changes were performed
344 twice weekly until the desired time in culture was reached (DIV20), at which point cells
345 were transfected or lysed.

346

347 **Transfection**

348 hEK293T cells and primary cortical neurons were transfected using
349 Lipofectamine 2000 (Life Technologies, 11668019). Briefly, 3 μ l Lipofectamine 2000
350 was mixed with 1 μ g of each HA-ZNF804A (Origene, RG211363) or Myc-NT5C2
351 (Origene, RC200194) plasmid construct in DMEM:F12 (Sigma, D6421) or neurobasal
352 medium (primary cortical neurons only). DNA:Lipofectamine mixtures were incubated
353 in a 37°C/5% CO₂ atmosphere for 20 minutes before being added dropwise to plated
354 hEK293T cells or primary cortical neurons. Transfected hEK293 cells were then further
355 incubated in a 37°C/5% CO₂ atmosphere for 24-48 hours before being fixed for
356 immunocytochemistry or lysed for immunoblotting accordingly. Transfected primary
357 cortical neurons were incubated in a 37°C/5% CO₂ atmosphere overnight during
358 transfection, then transferred back to feeding media the following day to maintain their
359 viability before being fixed for immunocytochemistry or lysed for immunoblotting
360 accordingly 24 hours later.

361 Short interfering RNA (siRNA) mediated knockdown of *Zfp804a* (the rat
362 homolog of *ZNF804A*) in rat primary cortical neurons was conducted using the N-Ter
363 Nanoparticle siRNA Transfection System (Sigma: N2788) at DIV15 per manufacturer's
364 instructions. The siRNA targeted exon 2 of *Zfp804a* and all results were compared to
365 Blank (N-TER, no transfection), Scramble (negative control) conditions. Briefly,

366 neurobasal feeding media was removed and replaced with neurobasal transfection
367 media (containing all feeding media components, but without penicillin/streptomycin)
368 with 1X APV prior to transfection. For 3 ml media, (1 ml per condition), the following
369 concentrations were required: 14.04 μ l of siRNA dilution buffer (Sigma: N0413) was
370 added to 1 μ l Double stranded deoxyribonucleic acid (dsDNA): Blank (N-TER),
371 Scramble (negative control GC duplex, Thermo Scientific: 465372) or siRNA (Thermo
372 Scientific: HSS150613). In a separate mixture, 7.2 μ l N-TER was mixed with 37.8 μ l
373 nuclease free water. The transfection mixture and individual siRNA conditions were
374 vortexed for 30 seconds and spun down with a microcentrifuge. Finally, 15 μ l N-TER
375 transfection mixture was added to each of the conditions, vortexed, spun down and
376 kept in the dark for 20 minutes at room temperature. Each condition was added
377 dropwise to the relevant coverslips and incubated at 37°C/5% CO₂ for 5 days prior to
378 immunocytochemistry.

379 siRNA mediated knockdown of *Nt5c2* in rat primary cortical neurons was
380 conducted using the Trilencer 27-mer NT5C2 siRNA kit (Origene: SR307908) at DIV15
381 per manufacturer's instructions. Briefly, primary cortical neurons were fed with 1X d,l
382 -APV in neurobasal feeding media for 30 minutes prior to transfection. SiRNA A (sense
383 sequence, 5'- UGAGAAGUAUGUAGUCAAGAUGGA -3') and siRNA B (sense
384 sequence, 5'- ACAACUGUAAUAGCUAUUGGUCUTC -3') conditions were compared
385 to Blank (N-TER, no transfection), Scramble (negative control sense sequence, 5'-
386 CGUUAUCGCGUAUAAUACGCGUAT-3'). N-TER was mixed with Opti-MEM (Life
387 Technologies: 31985-047) at a 1:50 ratio per manufacturer's instructions. Mixtures
388 were vortexed and spun down using a microcentrifuge, then kept in the dark for 30
389 minutes at room temperature. Each mixture was added dropwise to the relevant
390 coverslips and incubated at 37°C/5% CO₂ for 5 days prior to immunocytochemistry.

391

392 **Immunocytochemistry & Microscopy**

393 Rat primary cortical neurons and hEK293T cells were fixed in 4% sucrose and
394 4% formaldehyde for 10 minutes with agitation. Coverslips were washed in phosphate
395 buffered saline (PBS) and then incubated in ice cold methanol for 10 minutes. Cells
396 were permeabilized in 0.1% Triton-X100 (Alfa Aesar, A16046) in PBS and blocked
397 simultaneously in 2% normal goat serum (NGS – Cell Signaling Technology, 5425) in
398 PBS for one hour with agitation. Coverslips were subsequently incubated with primary
399 antibodies diluted in 2% NGS+PBS in a humidified chamber overnight at 4°C. The
400 following day, coverslips were washed 3x in PBS for 15 minutes each and were
401 incubated with secondary antibodies diluted in 2% NGS+PBS in a humidified chamber
402 at room temperature for one hour. Coverslips were washed 3x in PBS for 15 minutes
403 each. Lastly, cells were counterstained using 4',6-Diamidino-2-Phenylindole (DAPI –
404 Life Technologies, D1306) diluted in PBS before being mounted on microscope slides
405 with ProLong Gold Antifade Mountant (Life Technologies, P36930) and left to dry for
406 48 hours prior to confocal imaging. Primary antibodies included anti-ZNF804A C2C3
407 rabbit polyclonal (GeneTex, GTX121178, 1:200), anti-NT5C2 mouse monoclonal
408 (Abnova, H00022978-M02, 1:200), anti-NT5C2 rabbit polyclonal (Abcam, ab96084,
409 1:750), anti-MAP2 chicken polyclonal (Abcam, ab92434, 1:1000), anti-PSD95 guinea
410 pig polyclonal (Synaptic Systems, 124014, 1:500), anti-GFP rabbit polyclonal
411 (Origene, TA150032, 1:10,000), anti-HA mouse monoclonal (BioLegend, 901503,
412 1:1000), and anti-Myc mouse monoclonal (BioLegend, 626802, 1:1000). Actin
413 filaments were stained using ActinGreen™ 488 (Life Technologies, R37110) or
414 ActinRed™ 555 (Life Technologies, R37112) ReadyProbes™ per manufacturer's
415 instructions. Secondary antibodies included Alexa Fluor 488 goat anti-rabbit (A11034,

416 1:750), Alexa Fluor 568 goat anti-mouse (A11031, 1:750), Alexa Fluor 633 goat anti-
417 guinea pig (A21105, 1:500), Alexa Fluor goat anti-chicken (A21449, 1:750) (all
418 Invitrogen), and Alexa Fluor 405 goat anti-chicken (Abcam, ab175675, 1:500).

419 All experiments were imaged using a Leica SP-5 confocal microscope using a
420 Plan-Apochromatic 63x 1.40 NA oil-immersion objective (Leica microsystems,
421 506210). Fluorophores were excited using a 100 mW Ar laser (458, 476, 488, 496,
422 514 nm lines), 10 mW Red He/Ne (633 nm), and 50 mW 405 nm diode laser. Z-stacks
423 of each cell were acquired for all conditions at 0.5 μ m step size using Leica Application
424 Suite – Advanced Fluorescence software (LAS-AF; v2.7.3) installed on a
425 corresponding desktop computer running Windows XP (Microsoft, SP3). All Z-stacks
426 were exported to ImageJ (<https://imagej.nih.gov/ij/> v1.51j 8) where maximum intensity
427 projections and background subtracted images were generated (Schneider et al.,
428 2012).

429

430 **Co-Immunoprecipitation, Cell Fractionation & Immunoblotting**

431 hEK293 cells transfected with GFP-ZNF804A, HA-ZNF804A, or Myc-NT5C2
432 were lysed in co-immunoprecipitation (co-IP) buffer consisting of 10 mM Tris; pH7.4,
433 150 mM NaCl, 1% Triton-X100, 0.1% SDS, 1% Deoxycholate, 5 mM EDTA combined
434 with a protease/phosphatase inhibitor cocktail consisting of 1 mM AEBSF, 10 μ g/ml
435 Leupeptin, 1 μ g/ml Pepstatin A, 2.5 μ g/ml Aprotinin, 0.5 M NaF, and 1%
436 serine/threonine phosphatase inhibitor cocktail #3 (Sigma, P0044). Detergent soluble
437 lysates were sonicated for 10 pulses at 35% power and centrifuged at 15,000 rpm for
438 15 minutes at 4°C to remove cell debris, samples were then placed on ice for 30
439 minutes. An input sample of 75 μ l was removed from the lysate and protein
440 concentration was assessed using a Pierce Bicinchoninic acid (BCA) protein assay kit

441 (Thermo Scientific, 10678484). Concomitantly, 50 µl magnetic Dyna Beads Protein A
442 (Invitrogen, 10002D) were washed in 500 µl tris buffered saline+0.05% NP40 wash
443 buffer containing 8 µl ZNF804A antibody or 8 µl control Rabbit immunoglobulin (IgG)
444 (Santa Cruz Biotechnology, sc-2027). Samples were incubated at 4°C for 3 hours on
445 a rotator before being placed in a DynaMag™-2 magnetic rack (Thermo Scientific,
446 12321D) and washed twice with TBS+NP40 wash buffer. 150-200 µl total lysate was
447 equally added to ZNF804A or control normal rabbit IgG-bound beads. The samples
448 were then left rotating overnight at 4°C. The following day, co-IP samples were
449 returned to the magnetic rack, 50 µl of flow through was removed, and underwent BCA
450 analysis to determine protein concentration. The beads were washed in TBS+NP40
451 wash buffer and resuspended in 50 µl Laemmli sample buffer (Bio-Rad Laboratories,
452 161-0737) which were subsequently boiled at 95°C for 5 minutes to denature.

453 Cell fraction samples were prepared as follows. Cortical tissue from four 16
454 week old male CD1 mice were homogenized in 10x v/w of homogenisation buffer (0.32
455 M sucrose, 1 mM NaHCO₃, 1 mM MgCl₂) using a glass Dounce tissue homogenizer
456 for 10 strokes. Samples were then centrifuged at 4°C and at 200 RCF for 5 minutes:
457 the nuclear fraction (P1) was discarded, and supernatant containing the extranuclear
458 cell fraction (S1) retained. An aliquot of the S1 fraction was then centrifuged at 14,000
459 RCF for 15 minutes to produce the cytosolic fraction (S2 - supernatant) and crude
460 synaptosomes (P2 – pellet) fractions. The P2 pellet was resuspended in 1% Triton X-
461 100 buffer (20% v/v Triton X-100) with inhibitors. A further aliquot from the
462 resuspended P2 fractions were then centrifuged at 14,000 RCF for 15 minutes:
463 supernatant contain the ‘lightly bound’ synaptic fraction (P2S); the pellet was
464 resuspended in homogenisation buffer and contained the ‘tightly bound’ synaptic
465 fraction (P2P). All samples were then stored at -80°C.

466 Samples were resolved by SDS-PAGE, transferred to a PVDF membrane and
467 blocked for 1 hour in 5% bovine serum albumin (Sigma, A7906) in TBS+0.01%
468 Tween20. Membranes were then immunoblotted with primary antibodies overnight at
469 4°C, followed by 3x 15 minute washes in TBS-T. Membranes were then incubated with
470 anti-mouse (Life Technologies, A16078, 1:10,000) or anti-rabbit (Life Technologies,
471 G-21234, 1:10,000) horseradish peroxidase (HRP) conjugated secondary antibodies
472 for 1 hour at room temperature, followed by 3x 15 minute washes in TBS-T.
473 Membranes were then incubated in Pierce electrochemiluminescence substrate
474 (Thermo Scientific, 170-5061) for 5 minutes and subsequently scanned using a Bio-
475 Rad ChemiDoc MP (Bio-Rad). Band intensity was quantified by densitometry using
476 Image Lab software (Bio-Rad, v6.0.1).

477

478 **Quantification & Statistical Analysis**

479 Dendritic spine puncta were quantified from secondary and tertiary dendrites of
480 microtubule associated protein 2 (MAP2) positive neurons. Images of 3 neurons per
481 condition per culture were analyzed of 6 biological replicate cultures, approximately
482 100 μm of the dendrite was selected from 2-3 different dendrites per image. The areas
483 of the dendrite and spine region (2 μm on either side of the dendrite) were traced
484 manually and thresholded to select puncta sizes of 0.08-2 μm^2 for analysis. Puncta
485 count within the dendritic region was compared to puncta count in the synaptic region
486 in synaptic localization, synaptic colocalization and knockdown experiments. All
487 images were background subtracted to exclude non-specific staining in ImageJ prior
488 to quantification.

489 All datasets were subjected to outlier detection using the ROUT method (robust
490 regression and outlier removal – (Motulsky and Brown, 2006)) in GraphPad Prism

491 (v8.0.2 – Windows, GraphPad Software, San Diego, California USA,
492 <http://www.graphpad.com>), detected outliers were removed from their corresponding
493 dataset. All datasets were also tested for normality using the D'Agostino & Pearson
494 normality test to identify which datasets required parametric or non-parametric
495 analyses (D'agostino et al., 1990). All statistical analyses used an alpha level of 0.05.
496 Non-parametric Mann-Whitney U test was used to analyse all synaptic localisation and
497 synaptic colocalization data. Ordinary one-way analysis of variance (ANOVA) with
498 Bonferroni correction for multiple comparisons was used for analysing ZFP804A
499 puncta in ZFP804A knockdown experiments. Two-way ANOVA with Tukey's test for
500 multiple comparisons was used for analysing the effects of ZFP804A knockdown on
501 NT5C2 puncta. Two-way ANOVA with Tukey's test for multiple comparisons was also
502 used for analysing the effects of NT5C2 knockdown on ZFP804A puncta. All data are
503 shown as mean \pm standard error of the mean (SEM) and all error bars represent SEM.

504

505 **Acknowledgements**

506 This work was supported by grants from UK Medical Research Council, Grant No.
507 MR/L021064/1 to DPS; UK Medical Research Council Centre for Neurodevelopmental
508 Disorders (Grant No. MR/N026063/1); Royal Society UK (Grant RG130856) to DPS;
509 Independent Researcher Award from the Brain and Behavior Foundation (formally
510 National Alliance for Research on Schizophrenia and Depression (NARSAD) (Grant
511 No. 25957), awarded to D.P.S.; L.S. is supported by the UK Medical Research Council
512 (MR/N013700/1) and King's College London member of the MRC Doctoral Training
513 Partnership in Biomedical Sciences; P.R. was funded by a BBSRC-iCASE studentship
514 (BB/M503356/1); R.R.R.D. received funds from the Coordenação de Aperfeiçoamento

515 de Pessoal de Nível Superior (CAPES, BEX1279/13-0). We thank the Wohl Cellular
516 Imaging Centre for their help with imaging.

517

518 **Author Contributions**

519 A.A., L.S., N.J.F.G., P.R., M.R.J., L.T. and D.P.S. performed all experiments and
520 subsequent analysis. D.P.S., T.R.P. and R.R.R.D. designed the project and
521 experiments. A.A., N.J.F.G., and D.P.S. write the initial draft of the manuscript; A.,
522 L.S., N.J.F.G., P.R., M.R.J., L.T., T.R.P. and R.R.R.D. and D.P.S. edited and finalized
523 the manuscript.

524

525 **Conflict of interest**

526 The authors declare that they have no conflict of interest.

527

528 **References**

529

530 Amare, A.T., Vaez, A., Hsu, Y.-H., Direk, N., Kamali, Z., Howard, D.M., McIntosh, A.M.,
531 Tiemeier, H., Bültmann, U., Snieder, H., 2019. Bivariate genome-wide association
532 analyses of the broad depression phenotype combined with major depressive
533 disorder, bipolar disorder or schizophrenia reveal eight novel genetic loci for
534 depression. *Molecular psychiatry*, 1-10.

535 Birnbaum, R., Weinberger, D.R., 2017. Genetic insights into the neurodevelopmental
536 origins of schizophrenia. *Nature Reviews Neuroscience* 18, 727-740.

537 Cross-Disorder Group of the Psychiatric Genomics Consortium, 2013. Identification of
538 risk loci with shared effects on five major psychiatric disorders: a genome-wide
539 analysis. *Lancet* 381, 1371-1379.

540 D'agostino, R.B., Belanger, A., D'Agostino Jr, R.B., 1990. A suggestion for using
541 powerful and informative tests of normality. *The American Statistician* 44, 316-321.

542 Deans, P.M., Raval, P., Sellers, K.J., Gatford, N.J., Halai, S., Duarte, R.R., Shum, C.,
543 Warre-Cornish, K., Kaplun, V.E., Cocks, G., 2017. Psychosis risk candidate ZNF804A
544 localizes to synapses and regulates neurite formation and dendritic spine structure.
545 *Biological psychiatry* 82, 49-61.

546 Dong, F., Mao, J., Chen, M., Yoon, J., Mao, Y., 2021. Schizophrenia risk ZNF804A
547 interacts with its associated proteins to modulate dendritic morphology and synaptic
548 development. *Mol Brain* 14, 12.

549 Duarte, R.R., Bachtel, N.D., Côtel, M.-C., Lee, S.H., Selvackadunco, S., Watson, I.A.,
550 Hovsepian, G.A., Troakes, C., Breen, G.D., Nixon, D.F., 2019. The psychiatric risk
551 gene NT5C2 regulates adenosine monophosphate-activated protein kinase signaling
552 and protein translation in human neural progenitor cells. *Biological psychiatry* 86, 120-
553 130.

554 Duarte, R.R., Troakes, C., Nolan, M., Srivastava, D.P., Murray, R.M., Bray, N.J., 2016.
555 Genome-wide significant schizophrenia risk variation on chromosome 10q24 is
556 associated with altered cis-regulation of BORCS7, AS3MT, and NT5C2 in the human
557 brain. *American Journal of Medical Genetics Part B: Neuropsychiatric Genetics* 171,
558 806-814.

559 English, J.A., Fan, Y., Föcking, M., Lopez, L.M., Hryniewiecka, M., Wynne, K., Dicker,
560 P., Matigian, N., Cagney, G., Mackay-Sim, A., 2015. Reduced protein synthesis in
561 schizophrenia patient-derived olfactory cells. *Translational psychiatry* 5, e663-e663.

562 Forrest, M.P., Parnell, E., Penzes, P., 2018. Dendritic structural plasticity and
563 neuropsychiatric disease. *Nat Rev Neurosci* 19, 215-234.

564 Gandal, M.J., Zhang, P., Hadjimichael, E., Walker, R.L., Chen, C., Liu, S., Won, H.,
565 van Bakel, H., Varghese, M., Wang, Y., Shieh, A.W., Haney, J., Parhami, S., Belmont,
566 J., Kim, M., Moran Losada, P., Khan, Z., Mleczko, J., Xia, Y., Dai, R., Wang, D., Yang,
567 Y.T., Xu, M., Fish, K., Hof, P.R., Warrell, J., Fitzgerald, D., White, K., Jaffe, A.E.,
568 Psych, E.C., Peters, M.A., Gerstein, M., Liu, C., Iakoucheva, L.M., Pinto, D.,
569 Geschwind, D.H., 2018. Transcriptome-wide isoform-level dysregulation in ASD,
570 schizophrenia, and bipolar disorder. *Science* 362.

571 Hall, L.S., Medway, C.W., Pain, O., Pardinas, A.F., Rees, E.G., Escott-Price, V.,
572 Pocklington, A., Bray, N.J., Holmans, P.A., Walters, J.T.R., Owen, M.J., O'Donovan,
573 M.C., 2020. A transcriptome-wide association study implicates specific pre- and post-
574 synaptic abnormalities in schizophrenia. *Hum Mol Genet* 29, 159-167.

575 Hill, M.J., Bray, N.J., 2012. Evidence that schizophrenia risk variation in the ZNF804A
576 gene exerts its effects during fetal brain development. *American Journal of Psychiatry*
577 169, 1301-1308.

578 Hill, M.J., Jeffries, A.R., Dobson, R.J., Price, J., Bray, N.J., 2012. Knockdown of the
579 psychosis susceptibility gene ZNF804A alters expression of genes involved in cell
580 adhesion. *Hum Mol Genet* 21, 1018-1024.

581 Huang, Y., Huang, J., Zhou, Q.X., Yang, C.X., Yang, C.P., Mei, W.Y., Zhang, L.,
582 Zhang, Q., Hu, L., Hu, Y.Q., Song, N.N., Wu, S.X., Xu, L., Ding, Y.Q., 2020. ZFP804A
583 mutant mice display sex-dependent schizophrenia-like behaviors. *Mol Psychiatry*.

584 Jones, K.A., Eng, A.G., Raval, P., Srivastava, D.P., Penzes, P., 2014. Scaffold protein
585 X11alpha interacts with kalirin-7 in dendrites and recruits it to Golgi outposts. *J Biol*
586 *Chem* 289, 35517-35529.

587 Lewis, D.A., Levitt, P., 2002. Schizophrenia as a disorder of neurodevelopment.
588 Annual review of neuroscience 25, 409-432.

589 Mairet-Coello, G., Courchet, J., Pieraut, S., Courchet, V., Maximov, A., Polleux, F.,
590 2013. The CAMKK2-AMPK kinase pathway mediates the synaptotoxic effects of Abeta
591 oligomers through Tau phosphorylation. Neuron 78, 94-108.

592 Motulsky, H.J., Brown, R.E., 2006. Detecting outliers when fitting data with nonlinear
593 regression—a new method based on robust nonlinear regression and the false
594 discovery rate. BMC bioinformatics 7, 123.

595 O'Donovan, M.C., Craddock, N., Norton, N., Williams, H., Peirce, T., Moskvina, V.,
596 Nikolov, I., Hamshere, M., Carroll, L., Georgieva, L., 2008. Identification of loci
597 associated with schizophrenia by genome-wide association and follow-up. Nature
598 genetics 40, 1053-1055.

599 Penzes, P., Cahill, M.E., Jones, K.A., VanLeeuwen, J.-E., Woolfrey, K.M., 2011.
600 Dendritic spine pathology in neuropsychiatric disorders. Nature neuroscience 14, 285-
601 293.

602 Rapoport, J., Giedd, J., Gogtay, N., 2012. Neurodevelopmental model of
603 schizophrenia: update 2012. Molecular psychiatry 17, 1228-1238.

604 Ripke, S., Sanders, A.R., Kendler, K.S., Levinson, D.F., Sklar, P., Holmans, P.A., Lin,
605 D.-Y., Duan, J., Ophoff, R.A., Andreassen, O.A., 2011. Genome-wide association
606 study identifies five new schizophrenia loci. Nature genetics 43, 969.

607 Ripke, S., Walters, J.T., O'Donovan, M.C., 2020. Mapping genomic loci prioritises
608 genes and implicates synaptic biology in schizophrenia. 2020.2009.2012.20192922.

609 Schneider, C.A., Rasband, W.S., Eliceiri, K.W., 2012. NIH Image to ImageJ: 25 years
610 of image analysis. Nature methods 9, 671-675.

611 Schrode, N., Ho, S.M., Yamamuro, K., Dobbyn, A., Huckins, L., Matos, M.R., Cheng,
612 E., Deans, P.J.M., Flaherty, E., Barretto, N., Topol, A., Alganem, K., Abadali, S.,
613 Gregory, J., Hoelzli, E., Phatnani, H., Singh, V., Girish, D., Aronow, B.,
614 McCullumsmith, R., Hoffman, G.E., Stahl, E.A., Morishita, H., Sklar, P., Brennand,
615 K.J., 2019. Synergistic effects of common schizophrenia risk variants. *Nat Genet* 51,
616 1475-1485.

617 Singgih, E.L., van der Voet, M., Schimmel-Naber, M., Brinkmann, E.L., Schenck, A.,
618 Franke, B., 2021. Investigating cytosolic 5'-nucleotidase II family genes as candidates
619 for neuropsychiatric disorders in *Drosophila* (114/150 chr). *Transl Psychiatry* 11, 55.

620 Smeland, O.B., Frei, O., Dale, A.M., Andreassen, O.A., 2020. The polygenic
621 architecture of schizophrenia—Rethinking pathogenesis and nosology. *Nature*
622 *Reviews Neurology* 16, 366-379.

623 Srivastava, D.P., Woolfrey, K.M., Penzes, P., 2011. Analysis of dendritic spine
624 morphology in cultured CNS neurons. *JoVE (Journal of Visualized Experiments)*,
625 e2794.

626 Tao, R., Cousijn, H., Jaffe, A.E., Burnet, P.W., Edwards, F., Eastwood, S.L., Shin,
627 J.H., Lane, T.A., Walker, M.A., Maher, B.J., 2014. Expression of ZNF804A in human
628 brain and alterations in schizophrenia, bipolar disorder, and major depressive disorder:
629 a novel transcript fetally regulated by the psychosis risk variant rs1344706. *JAMA*
630 *psychiatry* 71, 1112-1120.

631 Topol, A., English, J., Flaherty, E., Rajarajan, P., Hartley, B., Gupta, S., Desland, F.,
632 Zhu, S., Goff, T., Friedman, L., 2015. Increased abundance of translation machinery
633 in stem cell-derived neural progenitor cells from four schizophrenia patients.
634 *Translational psychiatry* 5, e662-e662.

635 Williams, H.J., Norton, N., Dwyer, S., Moskvina, V., Nikolov, I., Carroll, L., Georgieva,
636 L., Williams, N.M., Morris, D.W., Quinn, E.M., 2011. Fine mapping of ZNF804A and
637 genome-wide significant evidence for its involvement in schizophrenia and bipolar
638 disorder. *Molecular psychiatry* 16, 429-441.

639 Zhou, D., Xiao, X., Li, M., 2020. The schizophrenia risk isoform ZNF804A(E3E4)
640 affects dendritic spine. *Schizophr Res* 218, 324-325.

641 Zhou, Y., Dong, F., Lanz, T., Reinhart, V., Li, M., Liu, L., Zou, J., Xi, H., Mao, Y., 2018.
642 Interactome analysis reveals ZNF804A, a schizophrenia risk gene, as a novel
643 component of protein translational machinery critical for embryonic
644 neurodevelopment. *Molecular psychiatry* 23, 952-962.

645

646 **Figure Legends**

647

648 **Figure 1 – NT5C2 and ZNF804A form a protein complex and co-localise when**
649 **expressed in hEK293 cells. (A)** Representative confocal image of hEK293T cells
650 expressing HA-ZNF804A and stained for F-actin. Ectopically expressed HA-ZNF804A
651 localises to cell cytoplasm and plasma membrane (yellow arrows). Near the plasma
652 membrane, HA-ZNF804A co-localises with F-actin. **(B)** Representative confocal
653 image of hEK293T cells expressing myc-NT5C2 and stained for F-actin. Ectopically
654 expressed myc-NT5C2 localises to cell cytoplasm (yellow arrows) similar to previous
655 descriptions. **(C)** Confocal images of untransfected hEK293T cells and cells co-
656 transfected with HA-ZNF804A and myc-NT5C2. In co-expressing cells, HA-ZNF804A
657 and myc-NT5C2 are found to co-localise to the cell cytoplasm and near the plasma
658 membrane (yellow arrows). Yellow dotted box indicates area magnified in (D). **(D) i) +**

659 **ii)** Intensity plot and magnified image of dotted box from (C), of co-localised HA-
660 ZNF804A and myc-NT5C2. **(E)** Co-immunoprecipitation (co-IP) assay of hEK293T
661 cells co-expressing HA-ZNF804A and myc-NT5C2. Cell lysates were
662 immunoprecipitated with a myc antibody to isolate NT5C2 and interacting partner.
663 Samples were subjected to immunoblotting and then subsequently probed with
664 antibodies for myc (to detect myc-NT5C2) and HA (to detect HA-ZNF804A). A specific
665 band for HA-ZNF804A was detected in co-IP'ed cell lysates expressing both proteins
666 but not from untransfected cell lysate. Scale bar = 5 μ m.

667

668 **Figure 2 – Synaptic localisation of ZNF804A and NT5C2 in cortical neurons. (A)**

669 Western Blotting of cell fractions generated from mouse cortex. S1, extranuclear cell
670 lysate; P2, crude synaptosomal fraction; S2 cytosol; P2S, synaptosomal supernatant,
671 P2P, synaptosomal precipitate. ZFP804A and NT5C2 were present in all fractions;
672 ZFP804A and NT5C2 was enriched in P2S compared to P2P fractions, whereas
673 NT5C2 was abundant in S2 fraction. PSD-95 was used to demonstrate synaptosomal
674 enrichment, and β -actin as a loading control. **(B)** Representative confocal image of a
675 section of dendrite from DIV20 cortical neurons immunostained for MAP2
676 (morphological marker) and a previously validated antibody for ZNF804A/ZFP804A.
677 Yellow arrows indicate localisation of ZFP804A along dendrites, whereas white arrow
678 heads indicate presence of protein in synaptic regions. Box and whisker plots, showing
679 maximum and minimum values, is of ZFP804A linear density in either dendrites or
680 synaptic region; n = 51 cells from 3 independent experiments. **(C)** Representative
681 confocal image of a section of dendrite from DIV20 cortical neurons immunostained
682 for MAP2 (morphological marker) and a previously validated antibody for NT5C2.
683 Yellow arrows indicate localisation of NT5C2 along dendrites, whereas white arrow

684 heads indicate presence of protein in synaptic regions. Box and whisker plots, showing
685 maximum and minimum values, is of NT5C2 linear density in either dendrites or
686 synaptic region; n = 51 cells from 3 independent experiments. Scale bar = 5 μ m.

687

688 **Figure 3 – NT5C2 and ZNF804A co-localise and form a protein complex near**

689 **synapses in cortical neurons. (A)** Representative confocal image of DIV 20 cortical

690 neurons immunostained for MAP2 (morphological marker), NT5C2 and ZFP804A.

691 Yellow arrows indicate co-localisation of NT5C2 and ZNF804A along dendrites,

692 whereas white arrow heads indicate co-localised puncta in synaptic regions. XZ and

693 YZ orthogonal view further demonstrate co-localisation of both proteins (orange

694 arrows). **(B and C)** Quantification of co-localisation: (B) density of NT5C2 puncta

695 positive for ZFP804A and (C) density of ZFP804A puncta positive for NT5C2 staining

696 along dendrites or within synaptic regions. N = 52 cells from 3 independent

697 experiments. **(D)** Co-immunoprecipitation (co-IP) assay of DIV 20 cortical neurons.

698 Cell lysates were immunoprecipitated with either an antibody against

699 ZNF804A/ZFP804A or against rabbit IgG (control). Samples were subjected to

700 immunoblotting and then subsequently probed with antibodies for NT5C2 and

701 ZNF804A. A specific band for ZNF804A was detected in the input, ZNF804A-IP and

702 flow through lanes as expected – no band was detected in the rabbit IgG-IP lane,

703 indicating the specificity of the assay. Probing with an antibody against NT5C2

704 revealed bands in the input, ZNF804A IP and flow through lanes, but not the rabbit

705 IgG-IP lane. This indicates that NT5C2 is part of a protein complex with ZNF804A.

706 Scale bar = 5 μ m.

707

708 **Figure 4 - Knockdown of *Zfp804a* causes the redistribution of NT5C2. (A)**

709 Representative confocal image of DIV20 cortical neurons either untransfected (blank)
710 or transfected with a scramble siRNA (scramble) or an siRNA for *Zfp804a* (*Zfp804a*
711 siRNA). Cells were immunostained for MAP2 (morphological marker) or with an
712 antibody against ZFP804A. Yellow arrows and white arrow heads indicate localisation
713 of ZFP804A along dendrites or within the synaptic region respectively. **(B)**
714 Quantification of ZNF804A linear density in Blank, scramble or *Zfp804a* siRNA
715 conditions. Box and whisker plots show minimum and maximum values of linear
716 density. N = 15-18 cells from 4 independent experiments. **(C)** Representative confocal
717 image of DIV20 cortical neurons, transfected as in (A). Cells were immunostained for
718 MAP2 and NT5C2. Yellow arrows and white arrow heads indicate localisation of
719 NT5C2 along dendrites or within the synaptic region respectively. **(D)** Quantification of
720 NT5C2 linear density in Blank, scramble or *Zfp804a* siRNA conditions. Box and
721 whisker plots show minimum and maximum values of linear density. N = 18 cells from
722 4 independent experiments. Scale bar = 5 μ m.

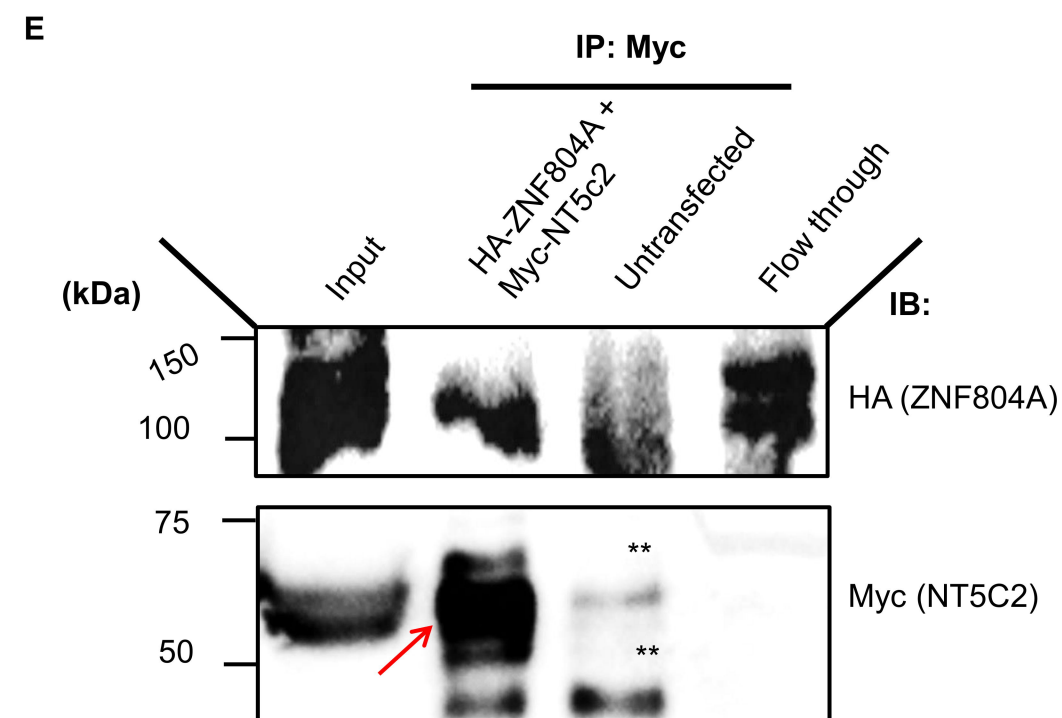
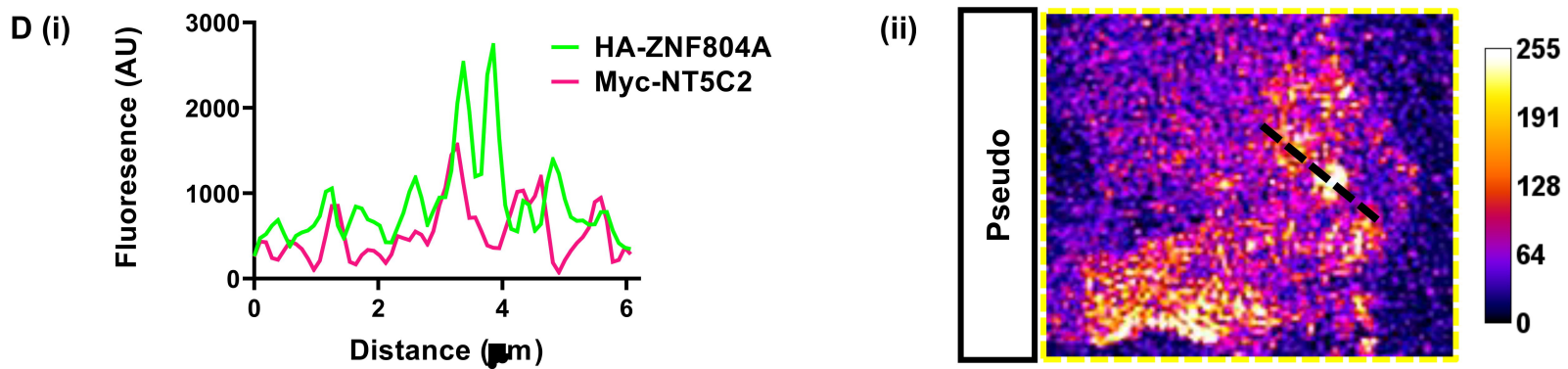
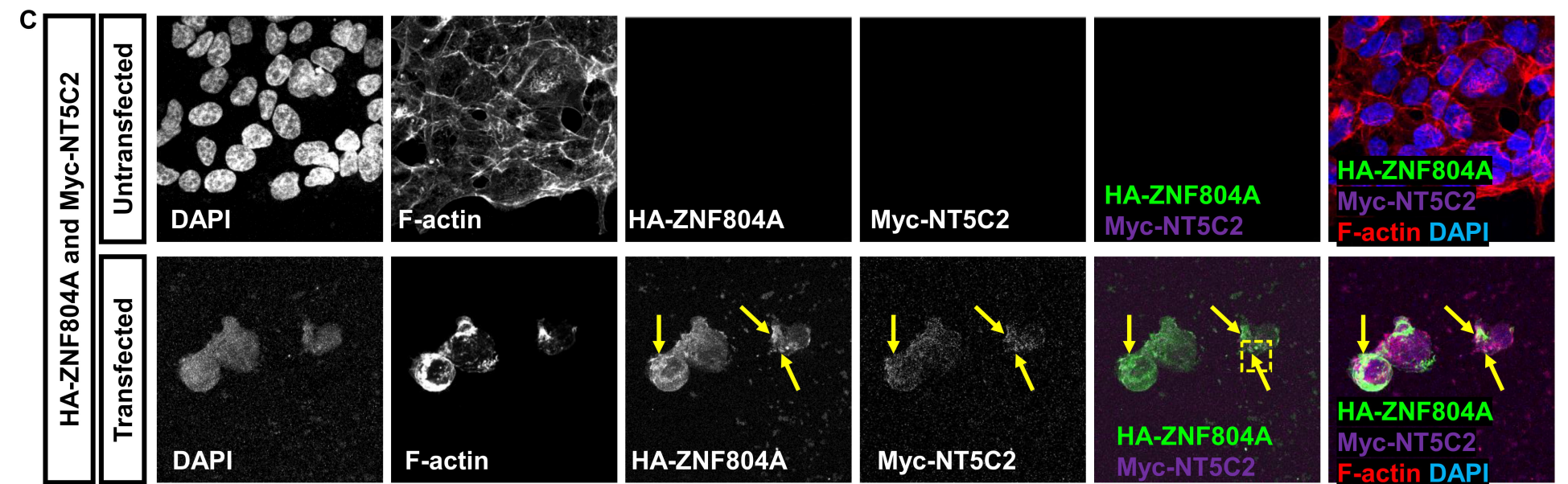
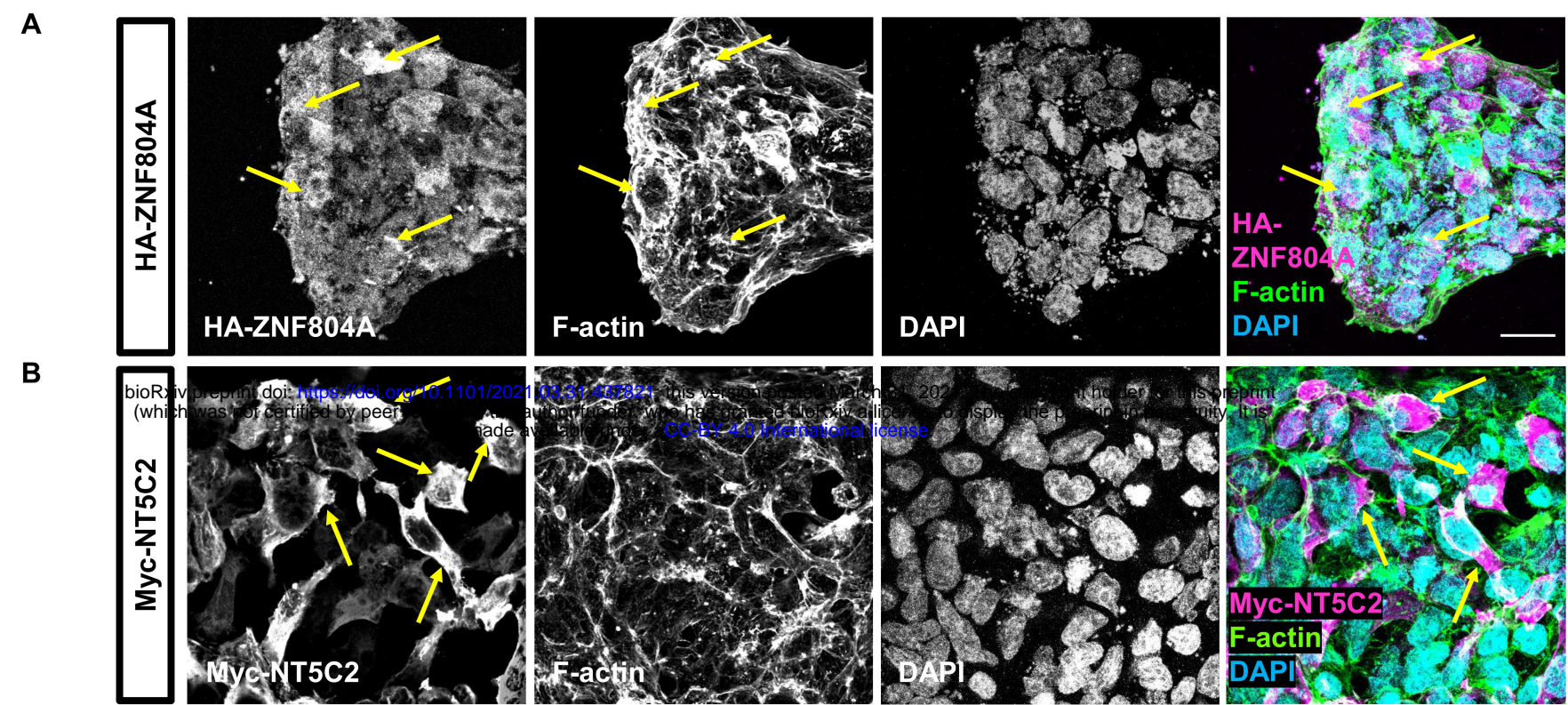
723

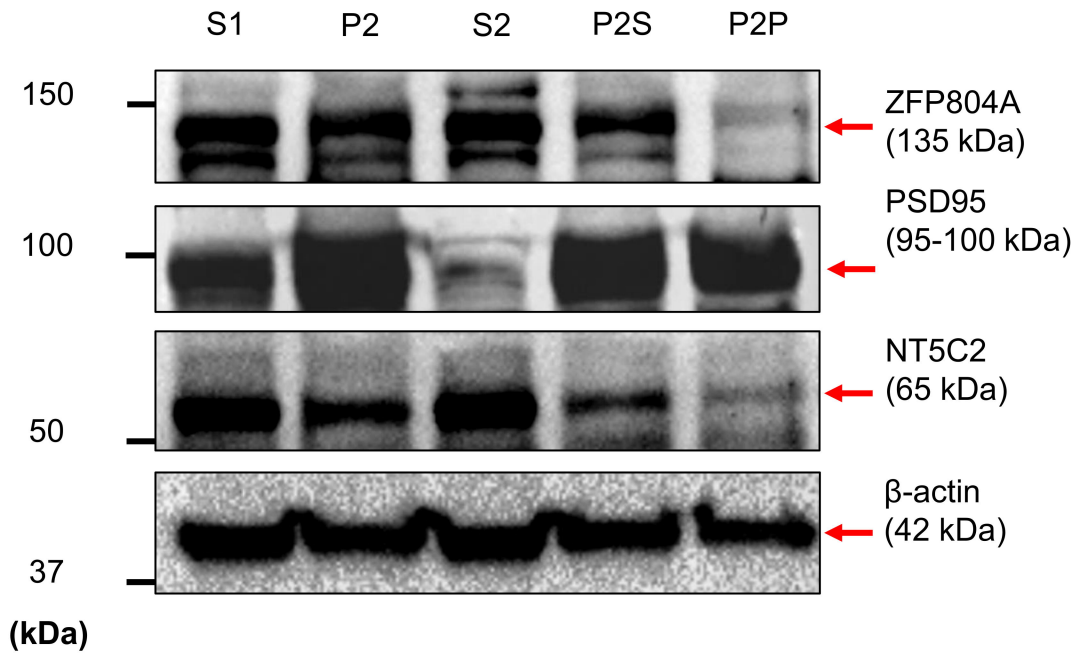
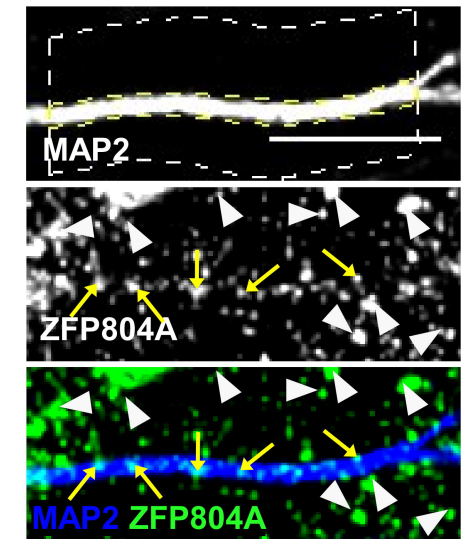
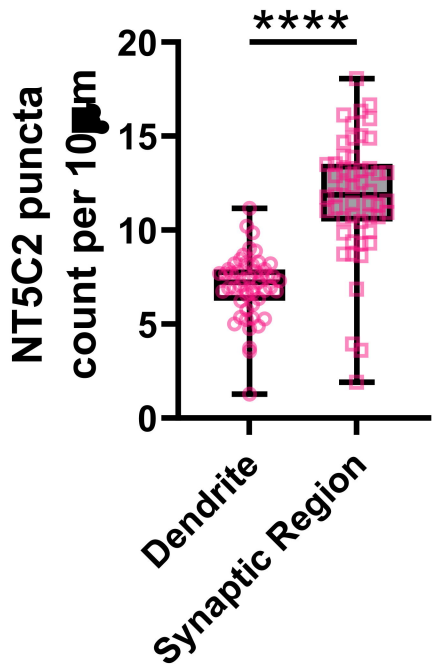
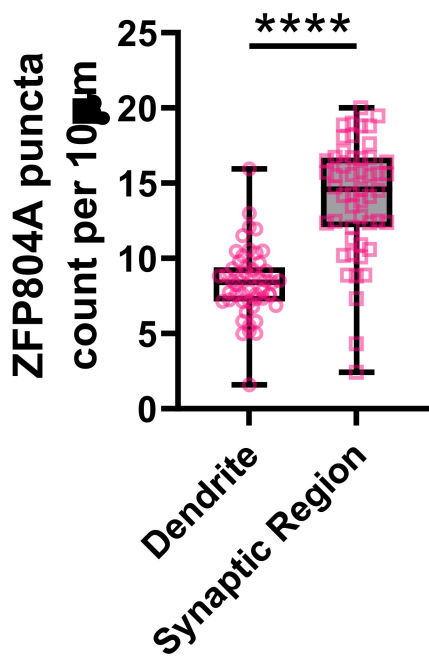
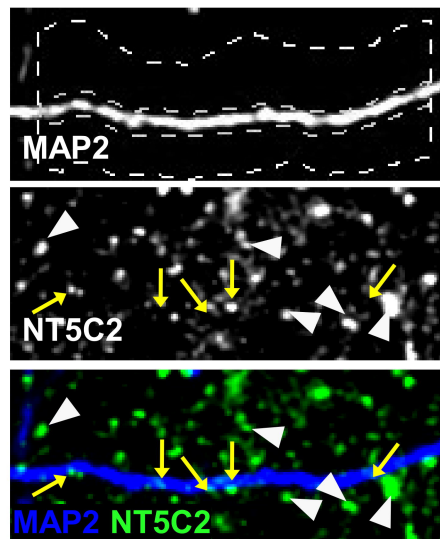
724 **Figure 5 - Knockdown of *Nt5c2* causes the redistribution of ZNF804A. (A)**

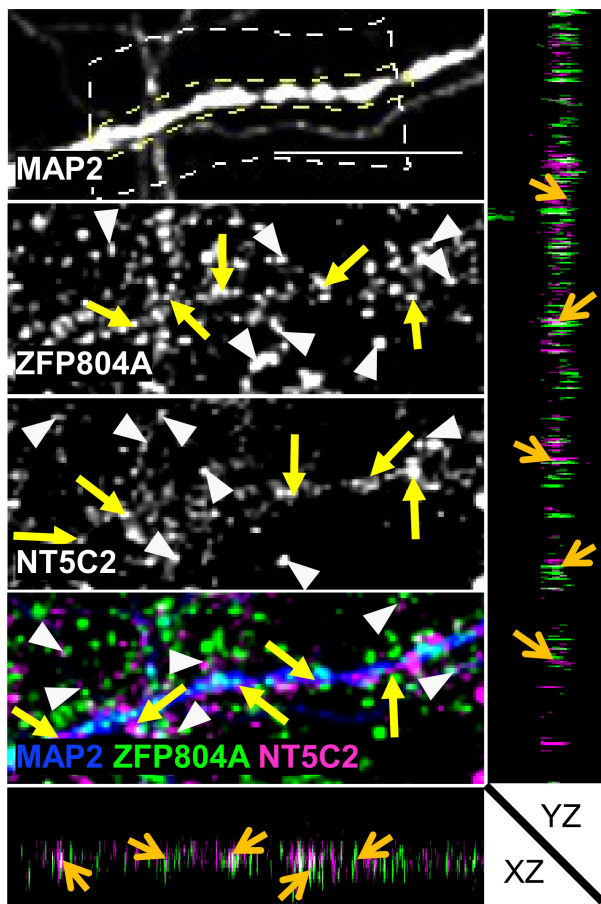
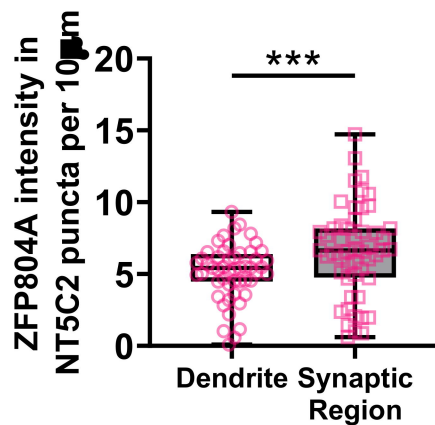
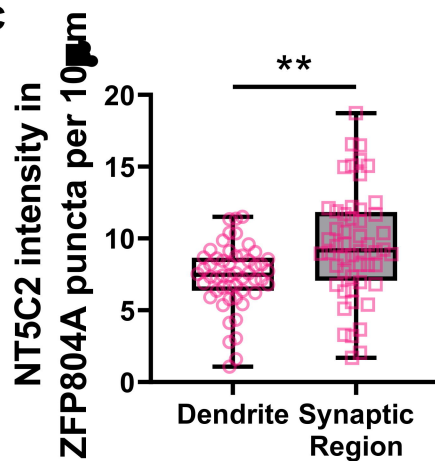
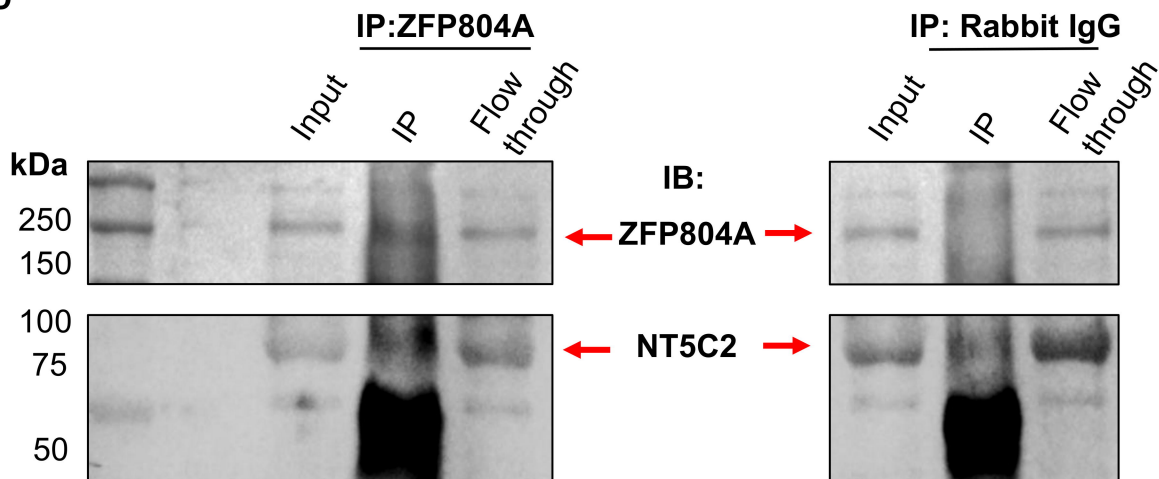
725 Western blotting of cell lysates from DIV20 cortical neurons either untransfected
726 (blank) or transfected with a scramble siRNA (scramble) or an siRNAs (A or B) for
727 *Nt5c2* (*Nt5c2* siRNA A or *Nt5c2* siRNA B). Immunoblots were probed with antibodies
728 against NT5C2 or β -actin (loading control). **(B)** Representative confocal image of
729 DIV20 cortical neurons, either untransfected (blank) or transfected with a scramble
730 siRNA (scramble) or an siRNA against *Nt5c2* (*Nt5c2* siRNA A). Cells were
731 immunostained for MAP2 and ZFP804A. Yellow arrows and white arrow heads
732 indicate localisation of ZFP804A along dendrites or within the synaptic region

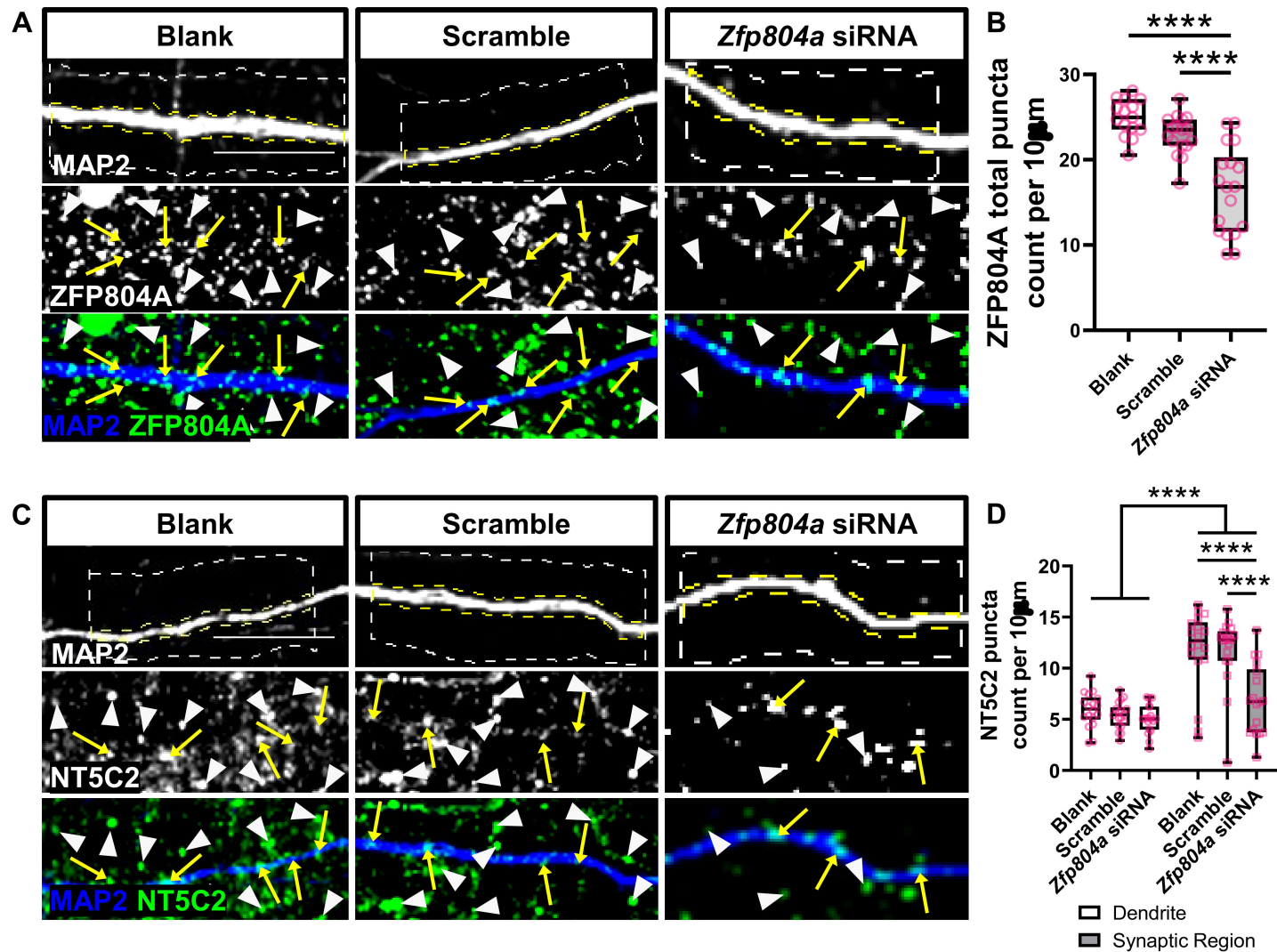
733 respectively. **(C)** Quantification of ZNF804A linear density in Blank, scramble or *Nt5c2*
734 siRNA A conditions. Box and whisker plots show minimum and maximum values of
735 linear density. N = 15 cells from 3 independent experiments. Scale bar = 5 μm .

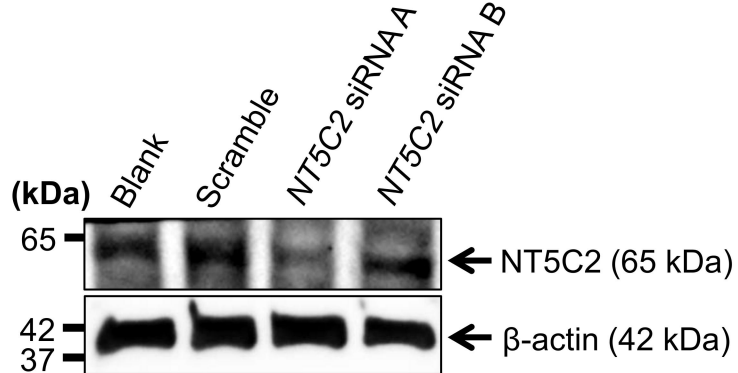
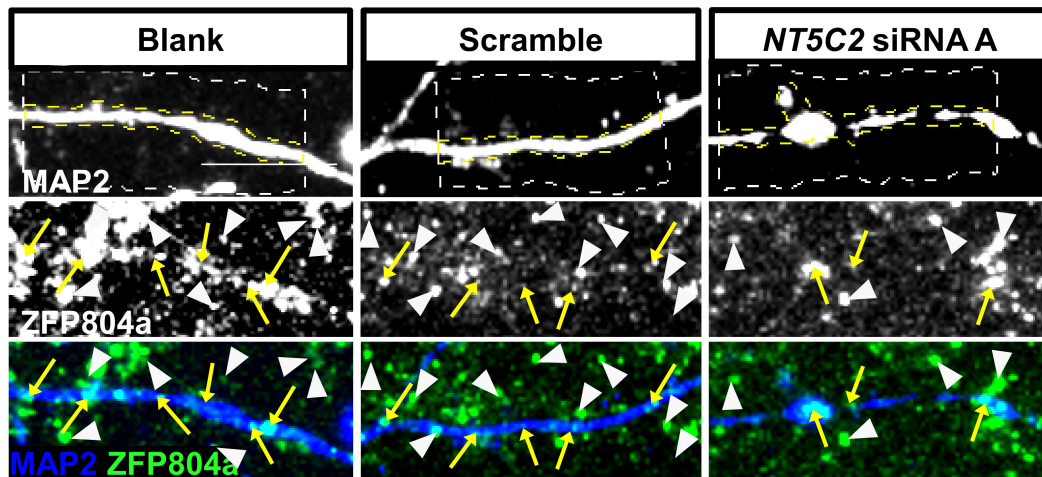
736



A**B****C**

A**B****C****D**



A**B****C**